PHYSICAL REVIEW E **90**, 052814 (2014)

Blind and myopic ants in heterogeneous networks

S. Hwang,[1,2] D.-S. Lee,[3,*] and B. Kahng[2,†]
[1]*Institute for Theoretical Physics, University of Cologne, 50937 Köln, Germany*
[2]*Department of Physics and Astronomy, Seoul National University, Seoul 151-747, Korea*
[3]*Department of Physics and Department of Natural Medical Sciences, Inha University, Incheon 402-751, Korea*

(Received 10 June 2014; revised manuscript received 27 October 2014; published 18 November 2014)

The diffusion processes on complex networks may be described by different Laplacian matrices due to heterogeneous connectivity. Here we investigate the random walks of blind ants and myopic ants on heterogeneous networks: While a myopic ant hops to a neighbor node every step, a blind ant may stay or hop with probabilities that depend on node connectivity. By analyzing the trajectories of blind ants, we show that the asymptotic behaviors of both random walks are related by rescaling time and probability with node connectivity. Using this result, we show how the small eigenvalues of the Laplacian matrices generating the two random walks are related. As an application, we show how the return-to-origin probability of a myopic ant can be used to compute the scaling behaviors of the Edwards-Wilkinson model, a representative model of load balancing on networks.

DOI: 10.1103/PhysRevE.90.052814 PACS number(s): 89.75.Fb, 05.40.Fb, 89.20.Hh

I. INTRODUCTION

Random walks in disordered media have been studied extensively to investigate a wide range of interesting topics including anomalous diffusion [1–3], the first passage time in searching problems and diffusion limited reactions [4–9], epidemic spreading [10–12], synchronization phenomena [13], the exploration and navigability of networks [14–21], and the community detection [22–25]. Various types of random-walk processes have been proposed since de Gennes coined the term "ant in the labyrinth" [26]. In particular, random walks of a blind ant and a myopic ant have attracted much attention. The transition matrix of a blind ant can be described as follows. As the blind ant at node i cannot see whether i and j are connected by a link or not, it blindly attempts to hop to an arbitrary node j with equal probability ϵ. Consequently the blind ant stays at i with probability $1-\epsilon k_i$ with k_i the number of neighbor nodes of node i. Consequently, ϵ is bounded as $\epsilon < 1/k_{\max}$, where $k_{\max}$ is the largest degree in the system. On the other hand, a myopic ant does not stay but always hops; it hops from a node i to a neighbor node j with probability $1/k_i$. The properties of the transition matrices and the occupation probabilities of both types of ants have long been studied [27,28]. In the stationary state, the occupation probability for each ant is given differently; it is identical at every node for blind ants [21,29], while it is proportional to the number of links of each node in case of myopic ants [30]. Despite such difference, it has been shown that the scaling behaviors of the mean square displacement and the diffusion time of both types of ants are in the same universality class on random percolating clusters [31,32].

During the last decades, scale-free topology of real-world networks has been identified from the World Wide Web to social and biological networks [33,34]. The abundance of hub nodes brings many interesting features of the dynamical processes on scale-free networks [35]. In particular, it was shown that the random walks of myopic ants on scale-free networks exhibit crossover behaviors of the return-to-origin (RTO) probability and that the Laplacian spectra of dense random scale-free networks have a gap [36–38]. One may wonder if such crucial heterogeneity of complex networks influences the case of blind ants as well.

In this paper we show analytically and numerically that the long-time behaviors of the occupation probabilities of blind and myopic ants are not different; however, rescaling of the occupation probability and time by node connectivity is needed appropriately. This finding leads us to find how the small eigenvalues of their transition matrices are related. The transition matrices of blind ants are used in the Edwards-Wilkinson model of the load balancing problem of underlying networks [39–42] and the Kuramoto model of synchronization phenomena in the strong-coupling limit [43]. We show how the scaling behaviors of the roughness and the synchronization order parameter in complex networks can be understood by the RTO probability of myopic ants displaying crossover behaviors [37].

II. OCCUPATION PROBABILITIES OF BLIND AND MYOPIC ANTS

The random walks of a blind ant and a myopic ant on an arbitrary undirected graph $\mathcal{G}$ of N nodes and Λ links are defined as follows. The adjacency matrix of $\mathcal{G}$ and the degree of each node i are denoted by A and k_i, respectively. Our study is restricted to sparse networks, the ones having finite mean connectivity $\langle k\rangle = 2\Lambda/N = O(1)$.

A blind ant at a node ℓ may stay there with probability $1-\epsilon k_\ell$ or hop to a neighbor node j with probability ϵ with ϵ being a parameter. Then the occupation probability $q_{ji}(\tau)$ at node j and τ time steps after starting at node i is evaluated as

$$q_{ji}(\tau) = (B^\tau)_{ji}, \quad B_{j\ell} = (1-\epsilon k_j)\delta_{j\ell} + \epsilon A_{j\ell}. \qquad (1)$$

To prevent the waiting probability $1-\epsilon k_i$ from being negative, we impose the condition $\epsilon < 1/\max(k_i)$.

On the other hand, a myopic ant at node ℓ hops to a neighbor node j with probability $1/k_\ell$. Therefore the occupation probability $p_{ji}(n)$ of a myopic ant at node j and n time steps

---

[*] deoksun.lee@inha.ac.kr
[†] bkahng@snu.ac.kr

after starting at node i is given by

$$p_{ji}(n) = (M^n)_{ji} = \sum_{\{i_2,i_3,\ldots,i_n\}} \prod_{\ell=1}^{n} \frac{A_{i_{\ell+1}i_\ell}}{k_{i_\ell}},$$
$$M_{j\ell} = \frac{A_{j\ell}}{k_\ell}, \tag{2}$$

where $i = i_1,i_2,\ldots,i_n,i_{n+1} = j$ denotes the sequence of the nodes visited by the myopic ant during n steps.

Each trajectory of a blind ant consists of waiting and hopping alternatively. Classifying the trajectories of a blind ant according to the number of hops n as $q_{ji}(\tau) = \sum_{n=0}^{\infty} q_{ji}^{(n)}(\tau)$, we find that the n-hop occupation probability $q_{ji}^{(n)}(\tau)$ of a blind ant is represented as

$$q_{ji}^{(n)}(\tau) = \begin{cases} B_{ii}^{\tau}\delta_{ij} & (n=0) \\ \sum_{\{i_2,i_3,\ldots,i_n\}} \sum_{\{\tau_1,\tau_2,\ldots,\tau_{n+1}\}} B_{jj}^{\tau_{n+1}} & \\ \times \prod_{\ell=1}^{n} \left(B_{i_{\ell+1}i_\ell} B_{i_\ell i_\ell}^{\tau_\ell}\right) \delta_{\sum_{\ell=1}^{n+1}\tau_\ell,\tau-n} & (n \geqslant 1) \end{cases}, \tag{3}$$

where $i = i_1,i_2,i_3,\ldots,i_n,i_{n+1} = j$ denotes the sequence of the nodes visited by the blind ant and τ_ℓ is the time spent at node i_ℓ. The diagonal (off-diagonal) elements of B represent the waiting (hopping) probabilities, and the quantity $B_{\ell'\ell}B_{\ell\ell}^{\tau}$ represents the probability that the blind ant stays at node ℓ for τ time steps and then hops to a neighbor node ℓ'.

Taking the limit $\epsilon \to 0$ and $\tau \to \infty$ with $t = \epsilon\tau$ fixed, the occupation probability of a blind ant can be considered as a function of continuous time t:

$$Q_{ji}(t) = \lim_{\epsilon\to 0} q_{ji}\left(\tau = \frac{t}{\epsilon}\right). \tag{4}$$

In Appendix A, we show that $Q_{ji}(t)$ is well defined in this limit.

In this continuous-time scheme, $B_{\ell'\ell}B_{\ell\ell}^{\tau} \to \epsilon e^{-k_\ell t}$ and the n-hop occupation probability is given by $Q_{ji}^{(0)}(t) = \delta_{ij}\exp(-k_j t)$ and for $n \geqslant 1$,

$$Q_{ji}^{(n)}(t) = \sum_{\{i_2,i_3,\ldots,i_n\}} \int dt_{n+1} \int \prod_{\ell=1}^{n} dt_\ell\, A_{i_{\ell+1}i_\ell} \times \exp\left(-\sum_{\ell=1}^{n+1} k_{i_\ell} t_\ell\right) \delta\left(\sum_{\ell=1}^{n+1} t_\ell - t\right). \tag{5}$$

The Laplace transform $\hat{Q}_{ji}^{(n)}(s) = \int_0^\infty dt\, Q_{ji}^{(n)}(t)\, e^{-st}$ is given by $\hat{Q}_{ji}^{(0)}(s) = \delta_{ij}/(k_j+s)$ for $n=0$ and for $n \geqslant 1$:

$$\hat{Q}_{ji}^{(n)}(s) = \frac{1}{(k_j+s)} \sum_{\{i_2,i_3,\ldots,i_n\}} \prod_{\ell=1}^{n} \frac{k_{i_\ell}}{k_{i_\ell}+s} \frac{A_{i_{\ell+1}i_\ell}}{k_{i_\ell}}. \tag{6}$$

Here the term $k_{i_\ell}/(k_{i_\ell}+s)$ is the Laplace transform of $k_{i_\ell}e^{-k_{i_\ell}t}$, which is the probability that the walker at node i_ℓ waits for t and hops to any of its neighbor nodes during time interval $dt = \epsilon^{-1}$. The term $A_{i_{\ell+1}i_\ell}/k_\ell$ describes the probability of hopping to a specific neighbor node $i_{\ell+1}$ under the condition that the walker hops between t and $t+dt$.

The term $\prod_{\ell=2}^{n} k_{i_\ell}/(k_{i_\ell}+s)$ in (6) depends on the degrees of the nodes lying on the path connecting i and j. To proceed, we assume that the degrees $k_{i_2},k_{i_3},\ldots,k_{i_n}$ are independent of one another. Then the degree distribution of the neighbor node of a node of degree k is independent of k, i.e., $P(k'|k) = \frac{kP_d(k)}{\langle k\rangle}$, given the degree distribution $P_d(k) = N^{-1}\sum_{i=1}^{N}\delta_{k_i,k}$ of a node. And for $n \gg 1$, we can use the central-limit theorem,

$$\prod_{\ell=2}^{n} \frac{k_{i_\ell}}{k_{i_\ell}+s} = \exp\left[(n-1)\left\langle \log\frac{k}{k+s}\right\rangle_{\rm link} + \sigma\sqrt{n-1}\,\xi\right], \tag{7}$$

where $\langle \log\frac{k}{k+s}\rangle_{\rm link}$ is the average of $\log\frac{k}{k+s}$ for the degree of the node at one end of a randomly chosen link, given by $\langle \log\frac{k}{k+s}\rangle_{\rm link} = \sum_k \frac{kP_d(k)}{\langle k\rangle}\log\frac{k}{k+s}$, and σ is its standard deviation $\sigma = \sqrt{\langle(\log\frac{k}{k+s})^2\rangle_{\rm link} - \langle\log\frac{k}{k+s}\rangle_{\rm link}^2}$. ξ can be considered as a random variable assigned to each path $\{i_2,\ldots,i_n\}$, and its distribution over different paths is assumed to satisfy $\langle\xi\rangle = 0$ and $\langle\xi^2\rangle = 1$ by the central limit theorem. We are interested in the large-t behavior of $Q_{ji}(t)$, which is related to the singular behavior of $\hat{Q}_{ji}(s)$ for small s. The small-s singularity of $\hat{Q}_{ji}(s)$ arises from summing the infinitely many large-n terms in $\hat{Q}_{ji}(s) = \sum_{n=0}^{\infty}\hat{Q}_{ji}^{(n)}(s)$. In Eq. (7), one can see that the first term is dominant over the second one in the right-hand side for $n \gg 1$. Expanding $\langle\log\frac{k}{k+s}\rangle_{\rm link}$ for small s as $\langle\log\frac{k}{k+s}\rangle_{\rm link} = \sum_{r=1}^{\infty}\frac{(-1)^r}{r}\langle(\frac{s}{k})^r\rangle_{\rm link} = -s\langle k^{-1}\rangle_{\rm link} + (1/2)s^2\langle k^{-2}\rangle_{\rm link} + O(s^3)$, we can approximate $\prod_{\ell=2}^{n}\frac{k_{i_\ell}}{k_{i_\ell}+s}$ in Eq. (7) by $e^{-s\langle k^{-1}\rangle_{\rm link}(n-1)}$. Then the remaining sum $\sum_{\{i_2,i_3,\ldots,i_n\}}\prod_{\ell=1}^{n}\frac{A_{i_{\ell+1}i_\ell}}{k_{i_\ell}}$ in Eq. (6) turns out to be equal to the occupation probability of a myopic ant $p_{ji}(n)$. Summing those approximated $\hat{Q}_{ji}^{(n)}(s)$'s for all $n \geqslant 1$ and using $\hat{Q}_{ji}^{(0)}(s) = \delta_{ij}/(k_j+s)$, we obtain

$$\hat{Q}_{ji}(s) \simeq \frac{\delta_{ij}}{k_j+s} + \frac{k_i}{(k_j+s)(k_i+s)} \sum_{n=1}^{\infty} e^{-(n-1)s\langle k^{-1}\rangle_{\rm link}} p_{ji}(n). \tag{8}$$

Even though the first few terms with small n in the summation should be corrected due to the fluctuation against the central limit theorem, the singular behavior of the summation for small s is due to the infinite sum of large-n terms and the corrections of the small-n terms do not affect it. Also the leading singular behavior of $\hat{Q}_{ji}(s)$ for small s is expected to come from the summation rather than the factor $1/(k_j+s)$ or $k_i/[(k_j+s)(k_i+s)]$, as the decaying behavior of $p_{ji}(n)$ is slower than any exponential function in most networks including the networks of finite spectral dimension d_s where $p_{ji}(n) \sim n^{-d_s/2}$ [5] and the random networks of $d_s \to \infty$, where $p_{ji}(n) \sim n^{-\xi}\exp(-\alpha n^{1/3})$ with α and ξ constants [29]. Therefore we have

$$\hat{Q}_{ji}(s) \simeq \frac{1}{k_j}\hat{p}_{ji}\left(e^{-s\langle k^{-1}\rangle_{\rm link}}\right), \tag{9}$$

where we introduced the generating function $\hat{p}_{ji}(z) = \sum_{n=0}^{\infty} z^n p_{ji}(n)$. Taking the inverse Laplace transform of Eq. (9), we find that the asymptotic behaviors of the occupation probabilities of two types of ants are related to each other by

$$Q_{ji}(t) \simeq \frac{\langle k\rangle}{k_j} p_{ji}(\langle k\rangle t), \tag{10}$$

where we used $\langle k^{-1}\rangle_{\text{link}} = 1/\langle k\rangle$. Equation (10) shows that the occupation probabilities of a blind ant and a myopic ant are identical in the long-time regime only if their time and probabilities are rescaled by the mean connectivity $\langle k\rangle$ and the degree k_j.

In the limit $t \to \infty$, Eq. (10) is always satisfied. As mentioned in Sec. I, the occupation probabilities of both ants in the limit $t \to \infty$ are known to be given by $Q_{ji}(t \to \infty) = N^{-1}$ and $p_{ji}(t \to \infty) = k_j/(2\Lambda)$, respectively [30], and thus Eq. (10) holds.

The validity of Eq. (10) for t finite but large depends on the validity of Eq. (9) as an approximation of Eq. (6). Approximating $\langle \log \frac{k}{k+s}\rangle_{\text{link}}$ in Eq. (7) by $-s\langle k^{-1}\rangle_{\text{link}}$ to obtain Eq. (8) and approximating $1/(k_j+s)$ and $1/(k_i+s)$ in Eq. (8) by $1/k_j$ and $1/k_i$, respectively, to obtain Eq. (9) can be justified for s small ($s \ll 1$). The resultant deviation between both sides of Eq. (10) may thus be small for t large ($t \gg 1$). On the other hand, Eq. (7) itself and dropping the term $\sigma\sqrt{n-1}\xi$ in Eq. (7) to obtain Eq. (8) are justified when the degrees of adjacent nodes are uncorrelated and n is large such that the central limit theorem yielding $\langle\xi\rangle = 0$ and $\langle\xi^2\rangle = 1$ is valid. The latter assumption is related to the topology of the considered network. (See Appendix B for the complete discussion.)

The leading behavior of $\hat{Q}_{ji}(s)$ for large s comes from $\hat{Q}^{(0)}_{ji}(s) = \delta_{ij}/(k_j+s)$, and thus the short-time behavior of $Q_{ji}(t)$ is given by $Q_{ji}(t) \simeq \delta_{ij}e^{-k_j t}$, implying that the blind walker is very likely to stay at the starting node for t small as shown in Appendix A.

We check the validity of Eq. (10) by numerical results. We simulate the random walks of the two kinds of ants on the Barabási-Albert (BA) model networks with its model parameter $m = 1$ and the (2,2) flower networks in the seventh generation [44,45], both of which are scale-free networks. In 1, it is shown that the occupation probability $p_{ji}(t)$ of myopic ants and the predicted one $\tilde{p}_{ji}(t) = \frac{k_j}{\langle k\rangle} Q_{ji}(\frac{t}{\langle k\rangle})$ from Eq. (10) by using $Q_{ji}(t)$ of blind ants are in good agreement for large t. Deviation between the RTO probabilities $p_{ii}(t)$ and $\tilde{p}_{ii}(t)$ is seen for small t, which is partly due to the term $\delta_{ij}/(k_j+s)$ dropped in Eq. (9), transformed to $\delta_{ij}e^{-k_i t}$ in the time domain, and is larger for k_i smaller. The time regime where $p_{ji}(t)$ and $\tilde{p}_{ji}(t)$ show a good agreement appears different in different networks and for different pairs of selected nodes i and j even in the same network. We define the relative deviation

$$\eta_{ji}(t) \equiv \frac{\tilde{p}_{ji}(t) - p_{ji}(t)}{p_{ji}(t)} \tag{11}$$

and measure it as a function of time for each case considered in Fig. 1, which is shown in Fig. 2. We find that $\eta_{ji}(t)$ decreases slowly with time without an identifiable characteristic time at which the deviation is significantly reduced. The magnitude and time dependence of $\eta_{ji}(t)$ seem to vary with the network topology and the two selected nodes i and j. Remarkably, the relative deviation seems decreasing with time in a way close to a power law t^{-1} in some of the considered cases. In Appendix B, we perform a detailed analysis of the correction terms arising from approximating Eq. (6) by Eq. (9) and show that the obtained correction terms can yield the t^{-1} decay of $\eta_{ji}(t)$ in uncorrelated networks of finite spectral dimension d_s. It is related to the neglected next leading-order terms in s in approximating Eq. (6) by Eq. (9).

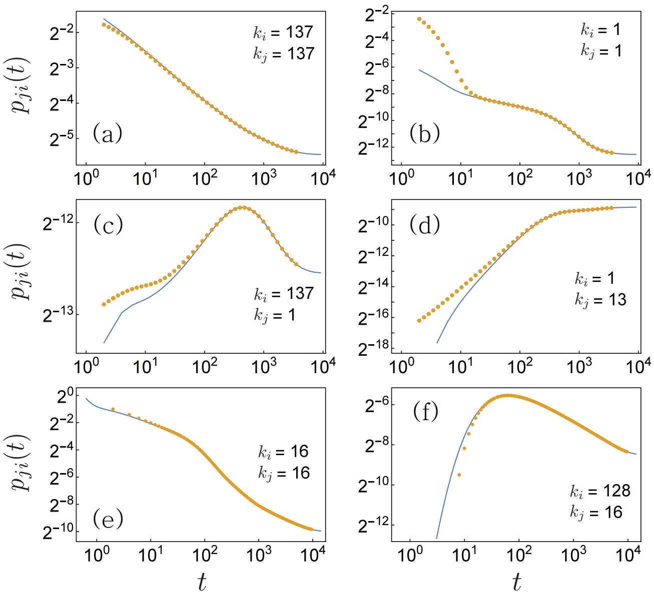

FIG. 1. (Color online) Comparison of the occupation probability $p_{ji}(t)$ of myopic ants (lines) and the predicted one $\tilde{p}_{ji}(t) = \frac{k_j}{\langle k\rangle} Q_{ji}(\frac{t}{\langle k\rangle})$ (points) from that of blind ants $Q_{ji}(t)$ and Eq. (10) in scale-free networks. (a) The RTO probability $p_{ii}(t)$ of myopic ants and its prediction $\tilde{p}_{ii}(t)$ made from $Q_{ji}(t)$ of blind ants in a BA network with $m = 1(\langle k\rangle = 2)$ and $N = 3000$. The spectral dimension is $d_s = 4/3$. The node i is the one selected randomly and has degree $k_i = 137$. (b) The RTO probabilities $p_{ii}(t)$ and $\tilde{p}_{ii}(t)$ in the same BA networks as in (a) for a different node i with $k_i = 1$. (c) The occupation probability $p_{ij}(t)$ and the predicted one $\tilde{p}_{ij}(t)$ in the same BA network with two selected nodes i and j having degrees $k_i = 137$ and $k_j = 1$, respectively. (d) $p_{ii}(t)$ and $\tilde{p}_{ii}(t)$ in the same BA networks with two selected nodes having degrees $k_i = 1$ and $k_j = 13$, respectively. (e) The RTO probabilities $p_{ii}(t)$ and $\tilde{p}_{ii}(t)$ in a (2,2) flower network in the seventh generation with $N = 10924$ and $\langle k\rangle = 3$. The spectral dimension is $d_s = 2$ and the selected node i has degree $k_i = 16$. (f) The occupation probabilities $p_{ij}(t)$ and $\tilde{p}_{ij}(t)$ in the same (2,2) flower network as in (e) for two selected nodes having degrees $k_i = 16$ and $k_j = 128$.

III. LAPLACIAN SPECTRA

The asymptotic equality in Eq. (10) suggests a relationship between the eigenvalues of the Laplacian matrices generating the random walks of myopic and blind ants. The transition matrices B and M in Eqs. (1) and (2) are represented in terms of two different Laplacian matrices L and $\tilde{L}$,

$$L_{ij} = k_i\delta_{ij} - A_{ij}, \ \ \tilde{L}_{ij} = \delta_{ij} - \frac{A_{ij}}{k_j}, \tag{12}$$

as $B_{ij} = \delta_{ij} - \epsilon L_{ij}$ and $M_{ij} = \delta_{ij} - \tilde{L}_{ij}$, respectively [36]. From Eqs. (1), (2), and (4), one can see that the occupation

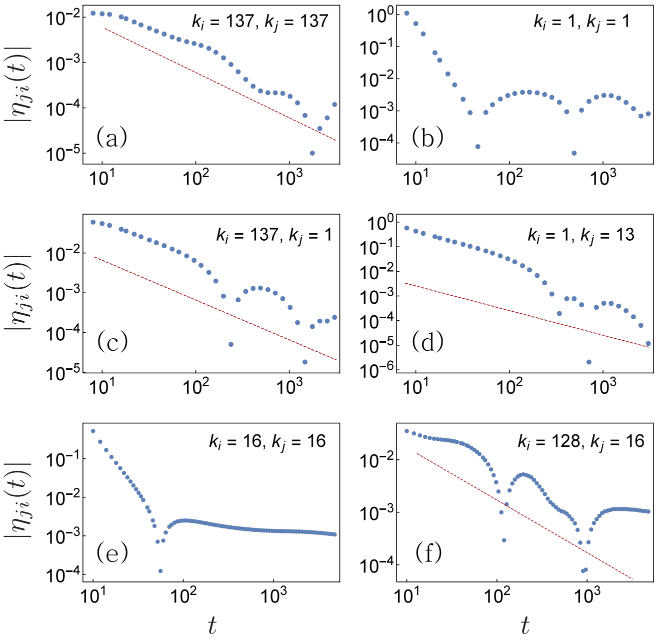

FIG. 2. (Color online) Plots of the relative deviation $\eta_{ji}(t) = \frac{\tilde{p}_{ji}(t) - p_{ji}(t)}{p_{ji}(t)}$ for each pair of selected nodes i and j, (a) $i = j$ with $k_i = 137$, (b) $i = j$ with $k_i = 1$, (c) $k_i = 137$ and $k_j = 1$, and (d) $k_i = 1$ and $k_j = 13$ in the BA network and (e) $i = j$ with $k_i = 16$ and (f) $k_i = 1$ and $k_j = 128$ in the (2,2) flower networks as considered in Fig. 1. The lines are guide for the eye, which have slope -1.

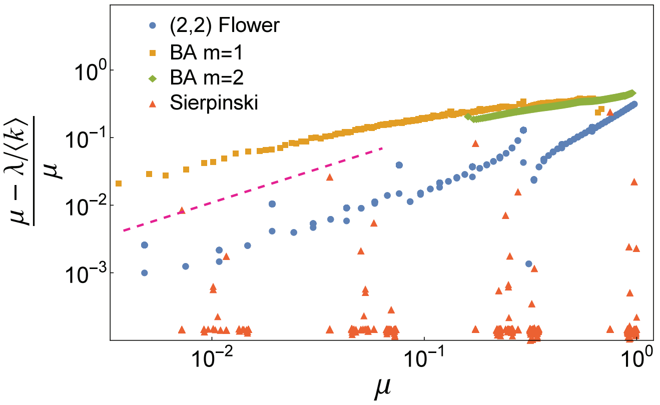

FIG. 3. (Color online) The relative deviation $\frac{\mu_r - \lambda_r/\langle k\rangle}{\mu_r}$ of the eigenvalues μ_r and λ_r of two Laplacian matrices L and $\tilde{L}$ in Eq. (12). The eigenvalues are obtained numerically for the model networks having different spectral dimensions d_s and the degree exponent γ: the (2,2) flower networks in the seventh generation ($N = 10924, \langle k\rangle = 3, d_s = 2, \gamma = 3$), the BA networks with $m = 1$ ($N = 16\,000, \langle k\rangle = 2, d_s = 4/3, \gamma = 3$) and $m = 2$ ($N = 16\,000, \langle k\rangle = 4, d_s \to \infty, \gamma = 3$), and the Sierpinski gasket in the eighth generation ($N = 9843, \langle k\rangle = 4, d_s = 2\log 3/\log 5, \gamma \to \infty$). The dashed line has slope 1.

probabilities are represented as

$$Q_{ji}(t) = (e^{-Lt})_{ji}, \quad p_{ji}(n) = ((I - \tilde{L})^n)_{ji}. \tag{13}$$

Note that we consider the random walk of blind ants in the continuous-time limit as in Eq. (4).

Suppose that λ_r and μ_r ($\ell = 1,2,\ldots,N$) are the rth smallest eigenvalues of L and $\tilde{L}$, respectively. Note that $\lambda_1 = \mu_1 = 0$ as $\sum_i L_{ij} = 0$ and $\sum_i \tilde{L}_{ij} = 0$. Then the occupation probabilities $Q_{ji}(t)$ and $p_{ji}(n)$ in Eq. (13) can be decomposed into these eigenmodes decaying with time as $e^{-\lambda_r t}$ and $e^{-\mu_r t}$ as

$$\begin{aligned} Q_{ji}(t) &= e_{ji}^{(1)}\left[1 + \sum_{r=2}^{\infty} e^{-\lambda_r t}\frac{e_{ji}^{(r)}}{e_{ji}^{(1)}}\right], \\ \frac{\langle k\rangle}{k_j} p_{ji}(\langle k\rangle t) &= \frac{\langle k\rangle}{k_j}\tilde{e}_{ji}^{(1)}\left[1 + \sum_{r=2}^{\infty}(1 - \mu_r)^{\langle k\rangle t}\frac{\tilde{e}_{ji}^{(r)}}{\tilde{e}_{ji}^{(1)}}\right] \\ &\simeq \frac{\langle k\rangle}{k_j}\tilde{e}_{ji}^{(1)}\left[1 + \sum_{r=2}^{\infty} e^{-\mu_r\langle k\rangle t}\frac{\tilde{e}_{ji}^{(r)}}{\tilde{e}_{ji}^{(1)}}\right], \end{aligned} \tag{14}$$

where $e_{ji}^{(r)} = \langle j|r\rangle\langle r|i\rangle$ ($\tilde{e}_{ji}^{(r)} = \langle j|r\rangle\langle r|i\rangle$) is the multiplication of the jth and ith components of the right and left eigenvector of $L(\tilde{L})$ associated with $\lambda_r(\mu_r)$. The last line of the equation holds as $t \to \infty$. Note that $e_{ji}^{(1)} = N^{-1}$ and $\tilde{e}_{ji}^{(1)} = \frac{k_j}{2\Lambda}$, which leads to the agreement of the stationary-state probabilities $Q_{ji}(t \to \infty) = e_{ji}^{(1)} = N^{-1}$ and $\frac{\langle k\rangle}{k_j} p_{ji}(t \to \infty) = \frac{\langle k\rangle}{k_j}\tilde{e}_{ji}^{(1)} = N^{-1}$ for $t \gg \lambda_2^{-1}$. In the time regime $\lambda_2^{-1} \lesssim t \ll \lambda_3^{-1}$, $Q_{ji}(t)$ is represented as a function of $t\lambda_2$ since $Q_{ji}(t) \simeq N^{-1}[1 + e^{-\lambda_2 t}\frac{e_{ji}^{(2)}}{e_{ji}^{(1)}}]$. Equation (10) holds approximately in this time regime, which implies that $\frac{\langle k\rangle}{k_j} p_{ji}(\langle k\rangle t)$ should be represented as $\frac{\langle k\rangle}{k_j} p_{ji}(\langle k\rangle t) \simeq N^{-1}[1 + e^{-\mu_2\langle k\rangle t}\frac{\tilde{e}_{ji}^{(2)}}{\tilde{e}_{ji}^{(1)}}]$ with $\langle k\rangle\mu_2 \simeq \lambda_2$ and $\frac{\tilde{e}_{ji}^{(2)}}{\tilde{e}_{ji}^{(1)}} \simeq \frac{e_{ji}^{(2)}}{e_{ji}^{(1)}}$. Given those obtained relations of λ_2, μ_2 and their associated eigenvectors, we further find for $\lambda_3^{-1} \lesssim t \ll \lambda_4^{-1}$ that the approximate identify of $Q_{ji}(t) \simeq N^{-1}[1 + e^{-\lambda_2 t}\frac{e_{ji}^{(2)}}{e_{ji}^{(1)}} + e^{-\lambda_3 t}\frac{e_{ji}^{(3)}}{e_{ji}^{(1)}}]$ and $\frac{\langle k\rangle}{k_j} p_{ji}(\langle k\rangle t) \simeq N^{-1}[1 + e^{-\mu_2\langle k\rangle t}\frac{\tilde{e}_{ji}^{(2)}}{\tilde{e}_{ji}^{(1)}} + e^{-\mu_3\langle k\rangle t}\frac{\tilde{e}_{ji}^{(3)}}{\tilde{e}_{ji}^{(1)}}]$ implies $\langle k\rangle\mu_3 \simeq \lambda_3$ and $\frac{\tilde{e}_{ji}^{(3)}}{\tilde{e}_{ji}^{(1)}} \simeq \frac{e_{ji}^{(3)}}{e_{ji}^{(1)}}$. Repeating this inductive reasoning, we find that

$$\lambda_r \simeq \langle k\rangle\mu_r \tag{15}$$

and $\frac{e_{ji}^{(r)}}{e_{ji}^{(1)}} \simeq \frac{\tilde{e}_{ji}^{(r)}}{\tilde{e}_{ji}^{(1)}}$ for small eigenvalues. The relation $\lambda_r \simeq \langle k\rangle\mu_r$ is based on the asymptotic equality of λ_{r-1} and $\langle k\rangle\mu_{r-1}$, and therefore the deviation of both sides of Eq. (15) is expected to accumulate with increasing r.

The relative deviation $\frac{\mu_r - \lambda_r/\langle k\rangle}{\mu_r}$ numerically obtained for model networks is presented in Fig. 3. As μ_r decreases, the deviation is shown to decrease, supporting the validity of Eq. (15) for small μ_r. The relative deviation of the eigenvalues appears to grow linearly with μ for the BA network with $m = 1$ and the (2,2) flower network, which is related to the t^{-1} decay of the relative deviation $\eta_{ji}(t)$ in Fig. 2 and is discussed in Appendix B.

The relative deviation appears depending on the network topology. For instance, while the relative deviation becomes less than 10^{-1} for $\mu \lesssim 0.25$ in the (2,2) flower networks in the seventh generation, it does around $\mu_{\text{th}} \simeq 0.03$ in the BA networks with $m = 1$ as shown in Fig. 3. As the relative deviation between $p_{ji}(t)$ and $\tilde{p}_{ji}(t)$ in Fig. 2 is related to the difference between μ_r and $\lambda_r/\langle k\rangle$ via Eq. (14), the larger relative deviation between $p_{ji}(t)$ and $\tilde{p}_{ji}(t)$ in the BA network can be attributed to the larger deviation of the eigenvalues than in the flower networks. In the Sierpinski gasket, we find the relative deviation is quite small over a wide range of eigenvalues as all the nodes except for the three oldest ones have the same degree.

We remark that in contrast to other networks, the BA networks with $m = 2$ has the second smallest eigenvalue λ_2 not sufficiently small even for large $N(= 16\,000)$. With a large value of λ_2 for finite N, the random walk reaches the stationary state with relatively small numbers of steps as the term $e^{-\lambda_2 t}$ decays fast in Eq. (14). It has been shown that λ_2 approaches 0 in the thermodynamic limit $N \to \infty$ as long as the smallest degree is 1 or 2 [29].

IV. DISCUSSION

Given the heterogeneity of node connectivity characteristic of real-world complex networks, it is highly necessary to understand how the dynamical processes depend on the specific way the node heterogeneity is incorporated into the dynamics. In this work, we have found that the long-time behaviors of the two types of random walks, those of blind ants and myopic ants, in heterogeneous networks are identical only if time and probability are rescaled by node connectivity as in Eq. (10). This result for the long-time behaviors of the occupation probabilities of blind and myopic ants allows us to find that the small eigenvalues of the two Laplacian matrices L and $\tilde{L}$ governing the two kinds of random walks are proportional to each other.

As an application, we can use the known features of the random walk of myopic ants to understand the dynamical processes driven by the Laplacian L of blind ants. The Edwards-Wilkinson(EW) model [39,40] describes the load balancing network as well as the fluctuating interface under thermal noise. To be specific, the load variables $\{h_i\}$ assigned to the nodes evolve with time in the EW model by the following Langevin equation:

$$\frac{\partial h_i(t)}{\partial t} = -\sum_{j=1}^{N} L_{ij} h_j + \xi_i(t), \tag{16}$$

where $\xi_t(t)$ is a white noise applied to each node i satisfying $\langle \xi_i(t)\xi_j(t')\rangle = 2\delta(t-t')\delta_{ij}$.

One of the most interesting features of the EW model is the scaling behaviors of the load fluctuation at a node $w_i(t) = \sqrt{\langle (h_i(t) - \bar{h}(t))^2\rangle_{st}}$ with $\bar{h}(t) = N^{-1}\sum_{i=1}^{N} h_i(t)$ and $\langle \bullet \rangle_{st}$ meaning the ensemble average. The square root of the node-averaged load fluctuation $w(t) \equiv \sqrt{N^{-1}\sum_{i=1}^{N}(w_i(t))^2}$ is called the roughness [39]. The occupation probability $Q_{ij}(t)$ of a blind ant is the Green's function of Eq. (16). For an initial network with no loads, $h_j(0) = 0$ for all j, the height $h_i(t)$ is represented as

$$h_i(t) = \sum_j \int_0^t Q_{ij}(t-t')\xi_j(t')\,dt'. \tag{17}$$

Then, in the stationary state ($t \to \infty$), the load fluctuation $w_i(\infty)$ can be evaluated by using the occupation probability of a myopic ant in Eq. (10) as

$$\begin{aligned} w_i(\infty)^2 &= \int_0^\infty [Q_{ii}(t) - Q_{ii}(\infty)]\,dt \\ &\simeq \frac{1}{k_i}\int_0^\infty [p_{ii}(t) - p_{ii}(\infty)]\,dt. \end{aligned} \tag{18}$$

We have recently found the crossover behaviors of the RTO probability $p_{ii}(t)$ in scale-free networks with the degree exponent γ and the spectral dimension d_s, which are given by

$$p_{ii}(t) \sim \begin{cases} t^{-d_s^{(\mathrm{hub})}/2} & \text{for} \quad 1 \ll t \ll t_c(k_i), \\ k_i t^{-d_s/2} & \text{for} \quad t_c(k_i) \ll t \ll t_x, \\ \frac{k_i}{\langle k\rangle N} & \text{for} \quad t \gg t_x, \end{cases} \tag{19}$$

with the two time scales $t_c(k_i) \sim k_i^{2(\gamma-1)/d_s}$ and $t_x \sim N^{2/d_s}$ [37]. In the early-time regime, an anomalous dimension $d_s^{(\mathrm{hub})} \equiv d_s\frac{\gamma-2}{\gamma-1}$ characterizes the time decay of the RTO probability. Using Eq. (19) in Eq. (18) we can obtain the scaling behaviors of the load fluctuation,

$$w_i(\infty)^2 \sim \begin{cases} N^{2/d_s - 1} & (\mathrm{I}) \quad d_s < 2, \\ k_i^{-\alpha} & (\mathrm{II}) \quad 2 < d_s < d_c, \\ k_i^{-1} & (\mathrm{III}) \quad d_s > d_c, \end{cases} \tag{20}$$

where the parameters $\alpha = (1 - 2/d_s)(\gamma - 1)$ and $d_c \equiv 2(\gamma - 1)/(\gamma - 2)$ are introduced. It is noteworthy that the integral is essentially determined by the long-time behavior of $Q_{ii}(t)$ in the case of $d_s^{(\mathrm{hub})} \leqslant 2$ ($d_s < d_c$), and thus one can utilize Eq. (10). On the other hand, if $d_s^{(\mathrm{hub})} > 2$ ($d_s > d_c$), $Q_{ii}(t)$ in the early-time regime makes a dominant contribution to the integral, and we cannot use Eq. (10). Nevertheless, Eq. (20)

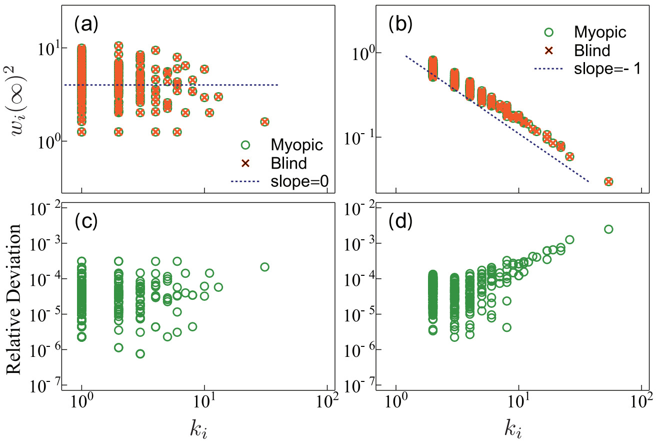

FIG. 4. (Color online) (a, b) The load fluctuations $\omega_i(\infty)^2$ on the BA networks with $m = 1$ and $m = 2$ as a function of degree k_i. As shown in Eq. (20), it follows the power law with the predicted exponents 0 and -1, respectively. The cross and open circle symbols indicate the exact results using the Laplacian L and the corresponding result using Eq. (10), respectively. Their relative deviation are shown in (c) for the BA network with $m = 1$ and (d) with $m = 2$. Even though the relative deviation seems to increase with k_i, it remains quite small in the entire range of k_i.

holds true since the integral converges to a finite constant independent of N. By averaging over all nodes i, we obtain the roughness $w_{st} = w(\infty)$ in the stationary state

$$w_{st}^2 \sim \begin{cases} N^{2/d_s-1} & \text{(I)} \quad d_s < 2, \\ \overline{k^{-\alpha}} & \text{(II)} \quad 2 < d_s < d_c, \\ \overline{k^{-1}} & \text{(III)} \quad d_s > d_c, \end{cases} \tag{21}$$

where the node average is denoted by $\overline{\bullet} = N^{-1}\sum_i \bullet$. This shows that the EW model presents a roughened load distribution in random networks with $d_s \leqslant 2$. Also, the local load fluctuation depends on the node degree if $d_s > 2$. In Fig. 4, we present the numerical results for the scaling behavior of the load fluctuation in for the BA networks with $m = 1 (d_s = 4/3)$ and $m = 2 (d_s \to \infty)$, which are in good agreement with Eq. (20).

The Kuramoto model for synchronization phenomena in heterogeneous networks is also described in terms of the Laplacian L in the strong-coupling limit. The similar analysis to the one we applied for the EW model allows us to see that the lower critical dimension of the Kuramoto model [43] is given in terms of the spectral dimension of the underlying network as $d_s = 4$ [46].

ACKNOWLEDGMENTS

This work was supported by the National Research Foundation of Korea (NRF) grants funded by the Korean Government (MSIP and MEST) [No. 2010-0015066 (B.K.) and No. 2013R1A2A2A01068845 (D.S.L.)].

APPENDIX A: RANDOM WALK OF BLIND ANTS IN THE CONTINUOUS-TIME LIMIT

In Eq. (1), we obtained the occupation probability $q_{ji}(\tau)$ in terms of the matrix $B_{j\ell} = (1 - \epsilon k_j)\delta_{j\ell} + \epsilon A_{j\ell}$. With the Laplacian L in Eq. (12), one can write $B = I - \epsilon L$, where I denotes the $N \times N$ identity matrix. If $\epsilon \ll 1$ and $\tau = t/\epsilon$ with t a fixed constant, one can see that

$$\begin{aligned} q_{ji}\left(\tau = \frac{t}{\epsilon}\right) &= ((I - \epsilon L)^\tau)_{ji} \\ &= \exp\left[-\tau\left(\epsilon L + \frac{1}{2}\epsilon^2 L^2 + \cdots\right)\right]_{ji} \\ &= \exp\left\{-tL\left[1 + O(\epsilon L)\right]\right\}_{ji}. \end{aligned} \tag{A1}$$

Therefore if we take the limit $\epsilon \to 0$ and $\tau \to \infty$ with $t = \tau/\epsilon$ fixed, the occupation probability in Eq. (A1) becomes a function of t defined as

$$Q_{ji}(t) \equiv \lim_{\epsilon \to 0} q_{ji}\left(\tau = \frac{t}{\epsilon}\right) = \exp(-tL)_{ji}. \tag{A2}$$

Equation (A1) suggests that $Q_{ji}(t)$ is well defined for all values of $t \in (0,\infty)$ as long as $\epsilon\lambda_r \ll 1$ for all $r = 1,2,\ldots,N$ with λ_r the eigenvalues of L. The condition is identical to $\epsilon \ll 1/\lambda_N$ given that $\lambda_1 = 0 < \lambda_2 \leqslant \lambda_3 \cdots \leqslant \lambda_N$. ϵ should also satisfy $\epsilon < 1/k_{\max}$ to prevent the transition probability B_{ij} from being negative. As $\lambda_N < 2k_{\max}$ [47], one can choose ϵ so that $\epsilon \ll 1/k_{\max}$. We remark that $Q_{ji}(t)$ in Eq. (A2) is the formal solution of the following continuous time Markov chain,

$$\frac{\mathrm{d}Q_{ji}(t)}{\mathrm{d}t} = -\sum_k L_{jk} Q_{ki}. \tag{A3}$$

From Eq. (A2), one can see that for t so small as $t \ll 1/k_i = 1/L_{ii}$, $Q_{ji}(t) \simeq \delta_{ij} - tL_{ij} = \delta_{ij} - tk_i\delta_{ij}$ and therefore

$$Q_{ji}(t) \simeq e^{-tk_i}\delta_{ji} = Q_{ji}^{(0)}(t),$$

implying that the probability of a random walker to experience one or more jumps for such small t is negligible. Note that the Laplace transform of $Q_{ji}(t)$ in this time regime is given by

$$\hat{Q}_{ji}^{(0)}(s) = \frac{\delta_{ij}}{k_j + s}. \tag{A4}$$

APPENDIX B: CORRECTION TERMS IN APPROXIMATING EQ. (6) BY EQ. (9)

Inserting Eq. (7) in Eq. (6) and using $\hat{Q}_{ji}(s) = \sum_{n=0}^{\infty} \hat{Q}_{ji}^{(n)}(s)$, one obtains

$$\begin{aligned} \hat{Q}_{ji}(s) = \frac{\delta_{ji}}{k_j + s} &+ \frac{k_i}{(k_j + s)(k_i + s)} \sum_{n=1}^{\infty} e^{-s(n-1)\langle k^{-1}\rangle_{\text{link}} + (1/2)s^2(n-1)\langle k^{-2}\rangle_{\text{link}} + O(s^3 n)} \\ &\times \sum_{i_2,\ldots,i_n} e^{s\sqrt{n-1}\sqrt{\langle k^{-2}\rangle_{\text{link}} - \langle k^{-1}\rangle_{\text{link}}^2}\,\xi + O(s^2\sqrt{n}\xi)} \prod_{\ell=1}^{n} \frac{A_{i_{\ell+1}i_\ell}}{k_{i_\ell}}, \end{aligned} \tag{B1}$$

where we used the expansion for σ appearing in Eq. (7) for small s as

$$\begin{aligned} \sigma^2 &\equiv \left\langle \left(\log\frac{k}{k+s}\right)^2 \right\rangle_{\text{link}} - \left\langle \log\frac{k}{k+s} \right\rangle_{\text{link}}^2 \\ &= \left(\langle k^{-2}\rangle_{\text{link}} - \langle k^{-1}\rangle_{\text{link}}^2\right) s^2 - \left(\langle k^{-3}\rangle_{\text{link}} - \langle k^{-1}\rangle_{\text{link}}\langle k^{-2}\rangle_{\text{link}}\right) s^3 + O(s^4). \end{aligned} \tag{B2}$$

In the sum over n in the right-hand side of Eq. (B1), the terms with $n \gg s^{-1}$ make little contribution due to the exponential term $e^{-s(n-1)\langle k^{-1}\rangle_{\text{link}}}$. For $n \lesssim s^{-1}$ and s small, other terms appearing in the exponents in Eq. (B1) are much less than 1. Utilizing the expansion $e^x \simeq 1 + x$ for small x, we can find that $\hat{Q}_{ji}(s)$ in Eq. (B1) can be approximated by Eq. (8) with the additional correction terms as

$$\hat{Q}_{ji}(s) \simeq \frac{\delta_{ji}}{k_j+s} + \frac{k_i}{(k_j+s)(k_i+s)} \sum_{n=1}^{\infty} e^{-(n-1)s\langle k^{-1}\rangle_{\rm link}} p_{ji}(n) + \hat{R}^{(\rm m)}_{ji}(s) + \hat{R}^{(xi)}_{ji}(s), \tag{B3}$$

where the leading correction terms are

$$\begin{aligned} \hat{R}^{(\rm m)}_{ji}(s) &= \frac{\langle k^{-2}\rangle_{\rm link}}{k_j} \sum_{n=1}^{\infty} e^{-s(n-1)\langle k^{-1}\rangle_{\rm link}} \frac{1}{2} s^2 (n-1) \sum_{i_2,\ldots,i_n} \prod_{\ell=1}^{n} \frac{A_{i_{\ell+1} i_\ell}}{k_{i_\ell}} \\ &= -\frac{1}{k_j} \frac{\langle k^{-2}\rangle_{\rm link}}{2\langle k^{-1}\rangle_{\rm link}} s^2 \frac{\partial}{\partial s} \bar{p}_{ji}(s\langle k^{-1}\rangle_{\rm link}), \\ \hat{R}^{(\xi)}_{ji}(s) &= \frac{\sqrt{\langle k^{-2}\rangle_{\rm link} - \langle k^{-1}\rangle^2_{\rm link}}}{k_j} \sum_{n=1}^{\infty} e^{-s(n-1)\langle k^{-1}\rangle_{\rm link}} s\sqrt{n-1} \sum_{i_2,\ldots,i_n} \xi_{i_2,\ldots,i_n} \prod_{\ell=1}^{n} \frac{A_{i_{\ell+1} i_\ell}}{k_{i_\ell}} \end{aligned} \tag{B4}$$

with

$$\bar{p}_{ji}(s) = \sum_{n=0}^{\infty} e^{-sn} p_{ji}(n+1). \tag{B5}$$

$\hat{R}^{(\rm m)}_{ji}(s)$ arises from approximating the mean value $\langle \log \frac{k}{k+s}\rangle_{\rm link}$ by $-\langle \frac{s}{k}\rangle_{\rm link}$ and $\hat{R}^{(\xi)}_{ji}(s)$ originates in neglecting the term $\sigma\sqrt{n-1}\xi$ in Eq. (7). While we assumed that s is small, as we are concerned in the large-t regime, for approximating $\langle \log \frac{k}{k+s}\rangle_{\rm link}$ by $-\langle \frac{s}{k}\rangle_{\rm link}$, the absence of correlation between the degrees of adjacent nodes on the paths connecting nodes i and j and the random distribution of the fluctuation ξ over different paths are assumed to neglect $\sigma\sqrt{n-1}\xi$. Therefore $\hat{R}^{(\xi)}_{ji}(s)$ depends on the network topology. Notice that $\bar{p}_{ji}(s)$ in Eq. (B5) and $\hat{p}_{ji}(e^{-s}) = \sum_{n=0}^{\infty} e^{-sn} p_{ji}(n)$ satisfy the relation $\bar{p}_{ji}(s) = e^{s}(\hat{p}_{ji}(e^{-s}) - \delta_{ij})$. Regarding the small-$s$ singularity, the factors $1/(k_i+s)$ and $1/(k_j+s)$ in front of the summation in Eq. (B3) are transformed to $e^{-k_i t}$ and $e^{-k_j t}$. Since we are interested in the large-t behavior of $Q_{ji}(t)$ that is expected to decay with time slower than such an exponential decay, we neglect those factors in the expressions for the correction terms in Eq. (B4). Let us denote Eq. (8), equal to the first and the second line of Eq. (B3), by $\hat{Q}^{*}_{ji}(s)$. Then Eq. (B3) is represented as $\hat{Q}_{ji}(s) = \hat{Q}^{*}_{ji}(s) + \hat{R}^{(\rm m)}_{ji}(s) + \hat{R}^{(\xi)}_{ji}(s)$. $\hat{Q}^{*}_{ji}(s)$ can be represented in terms of the generating function $\hat{p}_{ji}(e^{-s\langle k^{-1}\rangle {\rm link}}) = \sum_{n=0}^{\infty} e^{-sn\langle k^{-1}\rangle_{\rm link}} p_{ji}(n)$ as

$$\begin{aligned} \hat{Q}^{*}_{ji}(s) &= \frac{\delta_{ij}}{k_j+s} + \frac{k_i}{(k_j+s)(k_i+s)} e^{s\langle k^{-1}\rangle_{\rm link}} \\ &\quad \times \left[\hat{p}_{ji}\left(e^{-s\langle k^{-1}\rangle_{\rm link}}\right) - \delta_{ij}\right] \\ &= \frac{\delta_{ij}}{k_j+s}\left[1 - \frac{k_i e^{s\langle k^{-1}\rangle_{\rm link}}}{k_i+s}\right] \\ &\quad + \frac{k_i e^{s\langle k^{-1}\rangle_{\rm link}}}{(k_j+s)(k_i+s)} \hat{p}_{ji}\left(e^{-s\langle k^{-1}\rangle_{\rm link}}\right). \end{aligned} \tag{B6}$$

Using the expansion $e^{s\langle k^{-1}\rangle_{\rm link}} \simeq 1 + s\langle k^{-1}\rangle_{\rm link}$ and $\frac{1}{k_i+s} \simeq \frac{1}{k_i}(1-\frac{s}{k_i})$ for small s, we find that the leading singular behavior of $\hat{Q}^{*}_{ji}(s)$ is represented as

$$\hat{Q}^{*}_{ji}(s) \simeq \frac{1}{k_j} \hat{p}_{ji}\left(e^{-s\langle k^{-1}\rangle_{\rm link}}\right) + \hat{R}^{(p)}_{ji}(s) \tag{B7}$$

with the correction term $\hat{R}^{(p)}_{ji}(s)$ given by

$$\hat{R}^{(p)}_{ji}(s) = \frac{s}{k_j}\left(\langle k^{-1}\rangle_{\rm link} - \frac{1}{k_i} - \frac{1}{k_j}\right) \hat{p}_{ji}\left(e^{-s\langle k^{-1}\rangle_{\rm link}}\right). \tag{B8}$$

Therefore $\hat{Q}_{ji}(s)$ is represented in terms of that of a myopic ant $\hat{p}_{ji}(s)$ as

$$\hat{Q}_{ji}(s) \simeq \frac{1}{k_j} \hat{p}_{ji}\left(e^{-s\langle k^{-1}\rangle_{\rm link}}\right) + \hat{R}^{(\rm m)}_{ji}(s) + \hat{R}^{(\xi)}_{ji}(s) + \hat{R}^{(p)}_{ji}(s) \tag{B9}$$

with the correction terms given in Eqs. (B4) and (B8). Taking the inverse Laplace transform of $\hat{R}^{(\rm m)}_{ji}(s)$ and $\hat{R}^{(p)}_{ji}(s)$, we obtain that for t large,

$$\begin{aligned} R^{(\rm m)}_{ji}(t) &\simeq \frac{1}{k_j} \frac{\langle k^{-2}\rangle_{\rm link}}{2\langle k^{-1}\rangle^2_{\rm link}} \frac{\partial^2}{\partial t^2}\left[t p_{ji}\left(\frac{t}{\langle k^{-1}\rangle_{\rm link}} + 1\right)\right], \\ R^{(p)}_{ji}(t) &\simeq \frac{1}{k_j}\left(1 - \frac{k_i^{-1} + k_j^{-1}}{\langle k^{-1}\rangle_{\rm link}}\right) \frac{\partial}{\partial t}\left[p_{ji}\left(\frac{t}{\langle k^{-1}\rangle_{\rm link}}\right)\right]. \end{aligned} \tag{B10}$$

These two correction terms are given in terms of the derivatives of $p_{ji}(n)$. On the other hand, $R^{(\xi)}_{ji}(t)$ is not simply represented in terms of $p_{ji}(n)$ owing to the random variable ξ in Eq. (B4). If ξ is positive or negative randomly from path to path, the sum $\sum_{i_2,\ldots,i_n} \cdots$ in Eq. (B4) will be reduced considerably compared with that without ξ, and thus the contribution of $R^{(\xi)}_{ji}(t)$ will be smaller than $R^{(\rm m)}_{ji}(t)$ or $R^{(p)}_{ji}(t)$. However, the randomness of ξ could be violated depending on the network topology, and then $R^{(\xi)}_{ji}(t)$ would be considerable. The relative deviation considered in Eq. (11) is contributed to by the correction terms as $\eta_{ji}(t) = \eta^{(\xi)}_{ji}(t) + \eta^{(\rm m)}_{ji}(t) + \eta^{(p)}_{ji}(t)$ with

$$\eta^{(\xi)}_{ji}(t) = \frac{R^{(\xi)}_{ji}(t)}{p_{ji}(t)}, \quad \eta^{(\rm m)}_{ji}(t) = \frac{R^{(\rm m)}_{ji}(t)}{p_{ji}(t)}, \quad \eta^{(p)}_{ji}(t) = \frac{R^{(p)}_{ji}(t)}{p_{ji}(t)}. \tag{B11}$$

If $p_{ji}(t)$ decays with time t algebraically, $p_{ji}(t) \sim t^{-\theta}$ with θ a constant, which is the case for the RTO probability in the network of finite spectral dimension [37], then one can find that both $\eta_{ji}^{(\mathrm{m})}(t)$ and $\eta_{ji}^{(p)}(t)$ behave as

$$\eta_{ji}^{(\mathrm{m})}(t) \sim t^{-1}, \quad \eta_{ji}^{(p)}(t) \sim t^{-1} \tag{B12}$$

from Eq. (B10). Therefore the scaling behavior $\eta_{ji}(t) \sim t^{-1}$ shown in Fig. 2 may originate in that of $\eta_{ji}^{(\mathrm{m})}(t)$ and $\eta_{ji}^{(p)}(t)$. Such slow decay of the relative deviation implies the absence of a characteristic time scale at which the corrections are significantly reduced, except for the time at which the stationary state is achieved. In the stationary state, $p_{ji}(n)$ becomes constant, given by $k_j/(2L)$, and thus the correction terms in Eq. (B10) vanish, which is obvious from the validity of Eq. (10) in the $t \to \infty$ limit.

To see why the relative deviation $\frac{\mu - \frac{\lambda}{\langle k\rangle}}{\mu}$ is proportional to μ as observed in Fig. 3, suppose that the ordered eigenvalues μ_r of $\tilde{L}$ and λ_r of L are related to each other by

$$\mu_r = \frac{\lambda_r}{\langle k\rangle} + \Delta_r \tag{B13}$$

with Δ_r their deviation assumed to be small. Then the spectral density functions $\rho_\mu(\mu) = N^{-1}\sum_{r=2}^{N}\delta(\mu_r - \mu)$ and $\rho_\lambda(\lambda) = N^{-1}\sum_{r=2}^{N}\delta(\lambda_r - \lambda)$ are related to each other by $\rho_\mu(\mu) \simeq \langle k\rangle[\rho_\lambda(\langle k\rangle\mu) - \frac{\partial\rho_\lambda}{\partial\lambda}\langle k\rangle\Delta]$. Note that the spectral density functions are related to the occupation probabilities by the Laplace transformation, $p_{ji}(t) = p_{ji}(t \to \infty) + \frac{k_j}{\langle k\rangle}\int d\mu\rho_\mu(\mu)e^{-\mu t}\tilde{f}_{ji}(\mu)$ with $\tilde{f}_{ji}(\mu) \equiv N^{-1}\rho_\mu(\mu)^{-1}\sum_{r=2}^{N}\delta(\mu_r - \mu)\frac{\tilde{e}_{ji}^{(r)}}{\tilde{e}_{ji}^{(1)}}$, and $Q_{ji}(t)$ is similarly represented in terms of $\rho_\lambda(\lambda)$ with $f_{ji}(\lambda) \equiv N^{-1}\rho_\lambda(\lambda)^{-1}\sum_{r=2}^{N}\delta(\lambda_r - \lambda)\frac{e_{ji}^{(r)}}{e_{ji}^{(1)}}$ from Eq. (14). If we assume that $p_{ji}(t) \sim t^{-\theta}$ as above and $\tilde{f}_{ji}(\mu)$ does not exhibit a more dominant singular behavior than $\rho_\mu(\mu)$ for μ small, then $\rho_\mu(\mu) \sim \mu^{\theta-1}$ and $\rho_\lambda(\lambda) \sim \lambda^{\theta-1}$. It has been shown that large class of networks satisfy such properties [48]. Therefore the deviation of the occupation probabilities

$$\tilde{p}_{ji}(t) - p_{ji}(t) \sim \int d\lambda\frac{\partial\rho_\lambda}{\partial\lambda}\Delta e^{-\frac{\lambda}{\langle k\rangle}t}f_{ji}(\lambda) \tag{B14}$$

can behave as $t^{-1}p_{ji}(t) \sim t^{-\theta-1}$ only when

$$\Delta \sim \lambda^2, \tag{B15}$$

which means that the relative deviation $\frac{\mu - \frac{\lambda}{\langle k\rangle}}{\mu} \propto \mu$ as seen in Fig. 3.

---

[1] J.-P. Bouchaud and A. Georges, Phys. Rep. **195**, 127 (1990).

[2] B. D. Hughes, *Random Walks and Random Environments: Volume 1: Random Walks* (Oxford University Press, Oxford, 1995).

[3] R. Metzler and J. Klafter, Phys. Rep. **339**, 1 (2000).

[4] S. Redner, *A Guide to First-Passage Processes* (Cambridge University Press, Cambridge, 2001).

[5] S. Condamin, O. Benichou, V. Tejedor, R. Voituriez, and J. Klafter, Nature (London) **450**, 77 (2007).

[6] O. Bénichou and R. Voituriez, Phys. Rep. **539**, 225 (2014), from first-passage times of random walks in confinement to geometry-controlled kinetics.

[7] O. Bénichou, C. Chevalier, J. Klafter, B. Meyer, and R. Voituriez, Nat. Chem. **2**, 472 (2010).

[8] V. Sood, S. Redner, and D. ben Avraham, J. Phys. A **38**, 109 (2005).

[9] B. Meyer, C. Chevalier, R. Voituriez, and O. Bénichou, Phys. Rev. E **83**, 051116 (2011).

[10] R. Pastor-Satorras and A. Vespignani, Phys. Rev. Lett. **86**, 3200 (2001).

[11] A. Ganesh, L. Massoulie, and D. Towsley, in *INFOCOM 2005. 24th Annual Joint Conference of the IEEE Computer and Communications Societies. Proceedings IEEE*, Vol. 2 (IEEE, 2005) pp. 1455–1466.

[12] C. Castellano and R. Pastor-Satorras, Phys. Rev. Lett. **105**, 218701 (2010).

[13] A. Arenas, A. Díaz-Guilera, and C. J. Pérez-Vicente, Phys. Rev. Lett. **96**, 114102 (2006).

[14] J. M. Kleinberg, Nature (London) **406**, 845 (2000).

[15] S.-J. Yang, Phys. Rev. E **71**, 016107 (2005).

[16] L. da F. Costa and G. Travieso, Phys. Rev. E **75**, 016102 (2007).

[17] S. H. Lee and P. Holme, Phys. Rev. Lett. **108**, 128701 (2012).

[18] P. Yang, Q. Wang, and Z. Zheng, Phys. Rev. E **86**, 026203 (2012).

[19] M. Boguná, D. Krioukov, and K. C. Claffy, Nature Phys. **5**, 74 (2009).

[20] E. M. Bollt and D. ben-Avraham, New J. Phys. **7**, 26 (2005).

[21] M. De Domenico, A. Solé-Ribalta, S. Gómez, and A. Arenas, Proc. Natl. Acad. Sci. USA **111**, 8351 (2014).

[22] M. E. J. Newman and M. Girvan, Phys. Rev. E **69**, 026113 (2004).

[23] M. Rosvall and C. T. Bergstrom, Proc. Natl. Acad. Sci. USA **105**, 1118 (2008).

[24] H. Zhou, Phys. Rev. E **67**, 041908 (2003).

[25] S. Boccaletti, V. Latora, Y. Moreno, M. Chavez, and D.-U. Hwang, Phys. Rep. **424**, 175 (2006).

[26] P. G. de Gennes, La Recherche **7**, 919 (1976).

[27] G. Deutscher, *Percolation Structures and Processes (Annals of the Israel Physical Society)* (Institute of Physics, New York, 1983).

[28] D. ben-Avraham and S. Havlin, *Diffusion and Reactions in Fractals and Disordered Systems* (Cambridge University Press, Cambridge, 2005).

[29] A. N. Samukhin, S. N. Dorogovtsev, and J. F. F. Mendes, Phys. Rev. E **77**, 036115 (2008).

[30] J. D. Noh and H. Rieger, Phys. Rev. Lett. **92**, 118701 (2004).

[31] E. Seifert and M. Suessenbach, J. Phys. A **17**, L703 (1984).

[32] A. B. Harris, Y. Meir, and A. Aharony, Phys. Rev. B **36**, 8752 (1987).

[33] R. Albert, H. Jeong, and A.-L. Barabasi, Nature (London) **401**, 130 (1999).

[34] M. Newman, Contemp. Phys. **46**, 323 (2005).

[35] A. Barrat, M. Barthélemy, and A. Vespignani, *Dynamical Processes on Complex Networks* (Cambridge University Press, Cambridge, 2012).
[36] D. Kim and B. Kahng, Chaos **17**, 026115 (2007).
[37] S. Hwang, D.-S. Lee, and B. Kahng, Phys. Rev. E **85**, 046110 (2012).
[38] S. Hwang, D.-S. Lee, and B. Kahng, Phys. Rev. Lett. **109**, 088701 (2012).
[39] A.-L. Barabási and H. E. Stanley, *Fractal Concepts in Surface Growth* (Cambridge University Press, Cambridge, 1995).
[40] G. Korniss, M. A. Novotny, H. Guclu, Z. Toroczkai, and P. A. Rikvold, Science **299**, 677 (2003).
[41] B. Kozma, M. B. Hastings, and G. Korniss, Phys. Rev. Lett. **92**, 108701 (2004).
[42] H. Guclu, G. Korniss, and Z. Toroczkai, Chaos **17**, 026104 (2007).
[43] H. Hong, H. Park, and M. Y. Choi, Phys. Rev. E **72**, 036217 (2005).
[44] H. Rozenfeld, S. Havlin, and D. ben Avraham, New J. Phys. **9**, 175 (2007).
[45] M. Hinczewski and A. N. Berker, Phys. Rev. E **73**, 066126 (2006).
[46] S. Hwang, Ph.D. thesis, Seoul National University, Seoul, Korea, 2014.
[47] W. N. Anderson and T. D. Morley, Linear Multilinear Algebra **18**, 141 (1985).
[48] R. Burioni and D. Cassi, J. Phys. A **38**, R45 (2005).